

4. Zimmermann, U., Ehhalt, D. & Münnich, K.-O. *Proc. Symp. Isotopes in Hydrology*, Vienna, 567-584 (IAEA, Vienna, 1967).
5. Münnich, K.-O., Sonntag, C., Christmann, D. & Thoma, G. *Z. Mitt. Zentralinst. Isotopen Strahlenforschung* **29**, 319-332 (1980).
6. Allison, G. B. *J. Hydrol.* **55**, 163-169 (1982).
7. Barnes, C. J. & Allison, G. B. *J. Hydrol.* (in the press).
8. Allison, G. B., Barnes, C. J. & Hughes, M. W. *J. Hydrol.* (in the press).
9. Teller, J. T., Bowler, J. M. & Macumber, P. G. *J. geol. Soc. Aust.* **29**, 159-175 (1982).
10. Penman, H. L. *J. agric. Sci.* **30**, 437-462 (1940).
11. Harris, K. R., Mills, R., Back, P. J. & Webster, D. S. *J. magn. Reson.* **29**, 473-482 (1978).
12. de Vries, D. A. & Kruger, A. J. *Proc. C.N.R.S. Symp.*, Paris (1967).
13. Bureau of Meteorology *Climatic Atlas of Australia Map Set 3* (Australian Government, 1975).
14. Allison, G. B. & Hughes M. W. *J. Hydrol.* (in the press).

Latitudinal displacement from main moisture source controls $\delta^{18}\text{O}$ of snow in coastal Antarctica

David H. Bromwich* & Clark J. Weaver*†

* Institute of Polar Studies, The Ohio State University, Columbus, Ohio 43210, USA

† Atmospheric Sciences Program, The Ohio State University, Columbus, Ohio 43210, USA

$\delta^{18}\text{O}$ in polar precipitation is usually correlated with the condensation temperature^{1,2}. Here, observations of the oxygen isotopic composition of coastal Antarctic precipitation at Syowa Station^{3,4} during 1974 are re-evaluated, and it is demonstrated that monthly average $\delta^{18}\text{O}$ is more closely associated with the preceding month's mean temperature than that at the time of sampling. Linear regression indicates that the lag between temperature and isotopic ratio occurs because sea ice extent is a dominant factor for $\delta^{18}\text{O}$ values in Antarctic precipitation (Fig. 1). The annual growth and decay of Antarctic sea ice parallels the migration of the primary moisture source region which is located in the vicinity of the 0 or 1 °C sea surface isotherm. We conclude that the meridional distance from the primary moisture source is the main determinant of $\delta^{18}\text{O}$ values in coastal Antarctic precipitation.

Although it is widely known that long-term climatic information is recorded in the world's ice caps by the oxygen isotopic composition of past precipitation, relatively little effort has been devoted to understanding the atmospheric input signal. Koerner⁵ demonstrated that $\delta^{18}\text{O}$ values from the Queen Elizabeth Islands in Arctic Canada are linked with both the distance to the nearest appreciable moisture source and the elevation of sampling. The first factor appears to conflict with the well established multi-year relationship⁶ between $\delta^{18}\text{O}$ and temperature. Robin⁷ suggested that this contradiction can be resolved for Antarctica if temperature and displacement from the water vapour source are related. By using isotopic data^{3,4} from the coastal location at Syowa, where orographic influences are small, the relationships between $\delta^{18}\text{O}$ and both variables have been analysed and the results were found to confirm Robin's hypothesis.

The 1974 record of the $\delta^{18}\text{O}$ values in Syowa precipitation was investigated quantitatively by applying linear regression analysis on a monthly time scale. Of the 38 $\delta^{18}\text{O}$ measurements, 16 included some drift snow; such contamination does not appear to mask the $\delta^{18}\text{O}$ signal in precipitation⁴. For monthly average variables ($n = 11$), linear correlation coefficients of 0.6 ($r^2 = 0.36$) are significantly different from zero at the 95% confidence level.

The previous qualitative analysis of these data⁴ suggested that temperature of condensation (which theoretically is related to $\delta^{18}\text{O}$) is not the main factor controlling $\delta^{18}\text{O}$. Table 1 defines the three types of monthly temperature variables used in the present study: general (representing all conditions), precipitation, and δ -sampled. Figure 2 shows the erratic nature of $\hat{T}_p^{\delta^{18}\text{O}}$ compared with the smooth variation of $\delta^{18}\text{O}$ (except for August) and the other two temperature variables. This erratic

behaviour, which is shown by both the $\delta^{18}\text{O}$ -sampled surface and cloud temperature variables, means that they explain only a small percentage of the variance of $\delta^{18}\text{O}$ (see concurrent r^2 values in Table 1). This is in contrast to the higher degree of association between $\delta^{18}\text{O}$ and the concurrent precipitation and general temperature variables. Cloud temperatures approximate the condensation temperature rather than surface values, and thus correlate better with $\delta^{18}\text{O}$. However, because both the $\delta^{18}\text{O}$ sampled temperature variables have a weak association with $\delta^{18}\text{O}$, the temperature of condensation does not seem to be the principal determinant of $\delta^{18}\text{O}$.

Kato⁸ also found that the preceding month's mean temperature was more closely associated with $\delta^{18}\text{O}$ than the concurrent temperature. Comparison of both columns of the coefficients of determination (r^2) in Table 1 strongly support this observation. Note that the general temperature variables yield the best association with $\delta^{18}\text{O}$ when regression with the previous month's temperature is considered. In fact, any general temperature of the previous month taken at any standard level below 600 mbar is strongly associated with $\delta^{18}\text{O}$. Thus, $\delta^{18}\text{O}$ is more closely related to the atmospheric heat budget of the previous month as opposed to the temperature at the time of precipitation. This circumstance is masked when $\delta^{18}\text{O}$ and T_s are averaged over many years, and thus is not in conflict with the multiannual $\delta^{18}\text{O}$ -temperature relationship⁶ established for the present climate.

Sea ice growth to the north of Antarctica is delayed relative to air temperature by about a month and has been inferred as the cause for the higher $\delta^{18}\text{O}$ values between December and May in comparison to those for July–November⁴. Antarctic sea ice areas for 1974 have been derived from the passive microwave observations collected by the ESMR instrument onboard the NIMBUS 5 satellite⁹. Mid-month areas of sea ice between the longitudes 60° W and 90° E with ice concentrations of at least 15% and at least 85% were regressed with $\delta^{18}\text{O}$. Although results are independent of the longitudinal sector of sea ice considered (for example, the entire area of Antarctic sea ice yields similar results), the area with 15% or higher ice concentration explains 79% of the variance of $\delta^{18}\text{O}$ when the variables are in phase. When the areas of highly concentrated

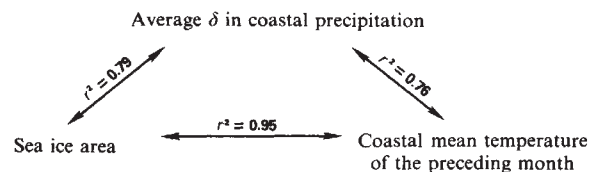


Fig. 1 Interrelationships between $\delta^{18}\text{O}$ (abbreviated as δ) in coastal precipitation, sea ice area and coastal mean temperature.

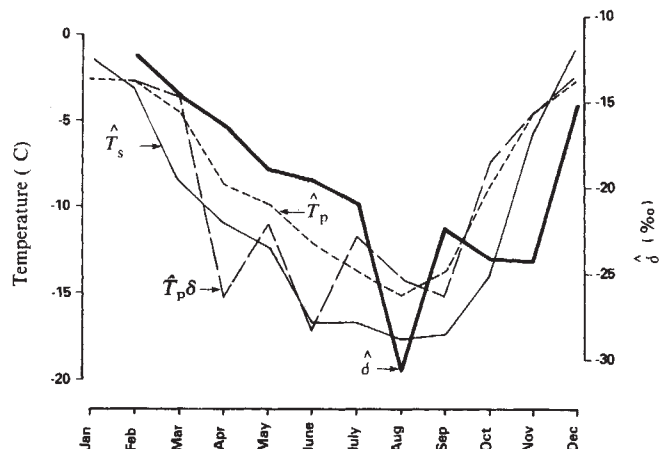


Fig. 2 Variations in \hat{T}_s , \hat{T}_p , $\hat{T}_p^{\delta^{18}\text{O}}$ and $\delta^{18}\text{O}$ during 1974 at Syowa Station.

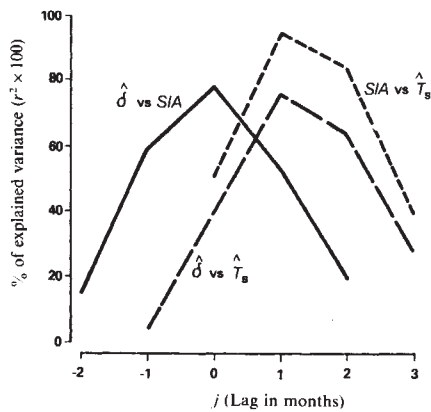


Fig. 3 Coefficients of determination (r^2) resulting from regressions:

- (a) $(\delta^{18}\text{O})^{i+j} = A + B(\hat{T}_s)^i$
 (b) $(\delta^{18}\text{O})^{i+j} = A + B(SIA)^i$
 (c) $(SIA)^{i+j} = A + B(\hat{T}_s)^i$

where i indicates the month and j specifies the lag in months in each of the regression equations. B is the regression derived slope of the line and A is the intercept. SIA is the area of sea ice with concentration $\geq 15\%$. An example of a positive lag ($j = 1$) is $\delta^{18}\text{O}$ for March compared with \hat{T}_s for February.

ice ($\geq 85\%$) are considered $\delta^{18}\text{O}$ and sea ice area variations are no longer in phase. This indicates that the origin of moisture being precipitated at Syowa is closer to the 15% ice concentration isopleth.

The interrelationships between sea ice area, mean temperature and $\delta^{18}\text{O}$ are summarized by Fig. 1. It is inferred that the physical control of $\delta^{18}\text{O}$ is related to the area of sea ice because their variations are in phase. The $\delta^{18}\text{O}$ -temperature correlation arises because temperature governs sea ice growth ($r^2 = 0.95$ when \hat{T}_s leads by 1 month the area of 15% or greater

ice concentration); the approximate 1 month lag between temperature forcing and sea ice response must be a consequence of the large thermal capacity of the ocean. A similar relationship between zonal averages of the latitude of the sea ice edge and the temperature was noted by Cavalieri and Parkinson¹⁰. Figure 3 depicts the change in the correlations between the variables as a function of lag, and demonstrates that the maximum percentage of explained variance is achieved by the relationships given in Fig. 1.

Additional support exists for the associations given in Fig. 1. The same strong lagged relationship between sea ice area and mean temperature at Syowa applies for 29 of the 36 months between 1973 and 1975 (7 months of sea ice data are missing). The $\delta^{18}\text{O}$ -lagged \hat{T}_s relationship holds for coastal Roi Baudouin^{2,11}; $\delta^{18}\text{O}$ values collected at Mizuho Camp (elevation 2,230 m and 270 km inland of Syowa) for part of 1974 also exhibit this behaviour¹². However, examination¹³ of the South Pole $\delta^{18}\text{O}$ data set¹ showed no evidence for a lag between $\delta^{18}\text{O}$ and temperature on a monthly time scale. The multiannual $\delta^{18}\text{O}$ -temperature diagram given by Dansgaard *et al.*¹⁴ also shows that the coastal areas and interior parts of Antarctica behave quite differently. Further research is needed to identify the physical basis of this apparent difference.

Robin⁷ suggested on the basis of Koerner's⁵ result for the Canadian Arctic that the sea ice effect found by Kato⁴ could be explained if the water vapour source region were represented by the position of the sea surface isotherms north of the pack ice limit; the most southerly isotherms undergo an annual migration in phase with that of the pack ice. Thus, the hypothesis is that the annual $\delta^{18}\text{O}$ variation in coastal precipitation is due to variations in the meridional distance between the source region and the precipitation site. In the immediate vicinity of Syowa Station, the area of sea ice within a given longitudinal sector is very nearly proportional to the meridional distance between the zonally averaged latitude of the sea ice edge and Syowa. Therefore, the present analysis indicates that $\delta^{18}\text{O}$ of

Table 1 Coefficients of determination (r^2) resulting from regression of monthly mean temperature variables[†] with $\delta^{18}\text{O}$ ($n = 11$) for Syowa Station in 1974

Variable	Definition	Concurrent r^2	Temperature leads by 1 month r^2
$\delta^{18}\text{O}$	Average of $\delta^{18}\text{O}$ values weighted by the estimated snowfall amount in each event	—	—
General temperatures	\hat{T}_{850} Monthly mean temperature at 850 mbar level	0.40	0.77
	\hat{T}_s Monthly mean temperature at surface	0.40	0.76
Precipitation temperatures	\hat{T}_{cl} Monthly mean cloud temperature* during precipitation	0.58	0.64
	\hat{T}_p Monthly mean surface temperature during precipitation	0.45	0.72
$\delta^{18}\text{O}$ -sampled precipitation temperatures	$\hat{T}_{cl}^{\delta^{18}\text{O}}$ Same as above \hat{T}_{cl} but only including temperatures during precipitation sampled for $\delta^{18}\text{O}$	0.20	—
	$\hat{T}_p^{\delta^{18}\text{O}}$ Same as above \hat{T}_p but only including temperatures during precipitation sampled for $\delta^{18}\text{O}$	0.19	—

[†] General temperatures are simple averages. The remaining four temperature averages (as well as $\delta^{18}\text{O}$) are weighted by the estimated snowfall amount of each precipitation event. The caret denotes a 1-month time average. Data are tabulated in ref. 17.

* Obtained by vertically averaging the temperature readings between the cloud boundaries (defined by saturation with respect to liquid water); weighting is with respect to water vapour mixing ratio.

Table 2 Regression analysis between $\delta^{18}\text{O}$ for Syowa in 1974* and the latitudinal distance (for the same month) from Syowa to the sea ice edge and to various sea surface isotherms ($n = 11$)

Monthly average independent variable [†] (km)	Ref.	Slope ± 1 s.e. (% km ⁻¹)	Intercept ± 1 s.e. (%)	r^2
Meridional distance to sea ice edge in 1974	18	-0.009 \pm 0.001	-13 \pm 1	0.82
Meridional distance to average sea ice edge 1972-77	19	-0.009 \pm 0.002	-12 \pm 1	0.80
Meridional distance to 0 °C isotherm [‡]	20	-0.007 \pm 0.001	-10 \pm 2	0.74
Meridional distance to 1 °C isotherm [‡]	20	-0.008 \pm 0.001	-7 \pm 2	0.75
Meridional distance to 2 °C isotherm [‡]	20	-0.014 \pm 0.002	+7 \pm 5	0.79

* The anomalous observed $\delta^{18}\text{O}$ value for August was replaced by the average of the July and September values.

[†] Zonally averaged between 20° and 60°E. Meridional distance is defined to be positive when measured northwards from Syowa.

[‡] Long-term average isotherm locations based on all available ship observations.

Syowa precipitation is in phase with and is linearly proportional to this distance.

To isolate the location of the water vapor source, the $\delta^{18}\text{O}$ record for Syowa was compared with the average for the same month of the meridional distance between Syowa and the following features: the pack ice edge and the 0, 1 and 2 °C sea surface isotherms. The results of this analysis are set out in Table 2. Unfortunately, only long-term average positions of the isotherms were available. The very similar results obtained when $\delta^{18}\text{O}$ was regressed against both the 1974 and 1972–77 sea ice edges suggest that the $\delta^{18}\text{O}$ versus 1974 isotherm comparison would not differ significantly from the isotope–isotherm analysis given in Table 2. A latitudinal isotopic gradient of $\sim 0.009\% \text{ km}^{-1}$ is compatible with the atmospheric water balance at Syowa Station (work in preparation). The much larger gradient obtained by Koerner⁵ of $0.02\% \text{ km}^{-1}$ may arise because the orography of the Queen Elizabeth Islands causes

more depletion of vapour¹⁵ (hence a more rapid decrease in $\delta^{18}\text{O}$) per km compared with the nonorographically induced precipitation over the pack ice upwind of Syowa. The intercept represents the $\delta^{18}\text{O}$ value of oceanic precipitation, which is implicitly assumed to be constant throughout the year. Aldaz and Deutsch¹ and Dansgaard⁶ pointed out that this may be -8% for latitudes in the vicinity of 50° S. We thus conclude that the primary origin of moisture being precipitated at Syowa lies in the vicinity of the 0 or 1 °C isotherm. On an annual basis, the corresponding average latitudes are 58° and 55° S, respectively; these source regions are poleward of those proposed previously^{1,16}. Accurate, simultaneous data probably will be needed to clarify the situation.

We thank Ian Whillans and Jeff Rogers for much assistance. The research was supported by NSF grants DPP 76-23428 and DPP 81-00142. This is contribution no. 464 of the Institute of Polar Studies, The Ohio State University.

Received 16 April; accepted 26 October 1982.

1. Aldaz, L. & Deutsch, S. *Earth planet. Sci. Lett.* **3**, 267–274 (1967).
2. Picciotto, E., De Maere, X. & Friedman, I. *Nature* **187**, 857–859 (1960).
3. Kato, K. *JARE Data Rep.* **36**, 156–167 (1977).
4. Kato, K. *Nature* **272**, 46–48 (1978).
5. Koerner, R. M. J. *Glaciol.* **22**, 25–41 (1979).
6. Dansgaard, W. *Tellus* **16**, 436–468 (1964).
7. Robin, G. de Q. *Proc. Canberra Symp.* 207–216 (IAHS Publ. No. 131, 1981).
8. Kato, K. *Antarctic Rec.* **67**, 124–135 (1979).
9. Zwally, H. J. et al. *4th NASA Weather and Climate Program Science Review* (ed. Kreins, E. R.) 335–340 (NASA, Washington DC, 1979).
10. Cavalieri, D. J. & Parkinson, C. L. *Mon. Weath. Rev.* **109**, 2323–2336 (1981).

11. Gonfiantini, R., Togliatti, V., Tongiorgi, E., De Breuck, W. & Picciotto, E. *J. geophys. Res.* **68**, 3791–3798 (1963).
12. Kato, K., Watanabe, O. & Satow, K. *Antarctic Res.* **67**, 136–151 (1979).
13. Bromwich, D. H. *Antarctic J. U.S.* (in the press).
14. Dansgaard, W., Johnsen, S. J., Clausen, H. B. & Gundestrup, N. *Medd. Gronland* **197**, 2 (1973).
15. Maxwell, J. B. *Arctic* **34**, 3, 225–240 (1981).
16. Friedman, I., Redfield, A. C., Schoen, B. & Harris, J. *Rev. Geophys.* **2**, 177–224 (1964).
17. Japan Meteorological Agency, *Antarctic Met. Data* **15**, 1–215 (1977).
18. Fleet Weather Facility, *Antarctic Ice Charts 1973–1974* (Suitland, Maryland, 1975).
19. Streten, N. A. & Pike, D. J. *Arch. Met. Geophys. Bioklim.* **A 29**, 279–299 (1980).
20. Keeley, J. R. & Taylor, J. D. *Data Products from First GARP Global Experiment* (Marine Environmental Data Service, Ottawa, 1981).

Reconstruction of Palaeogene climate from palynological evidence

R. N. L. B. Hubbard & M. C. Boulter

Faculty of Science, North East London Polytechnic, Romford Road, London E15 4LZ, UK

Multivariate statistical analysis of Palaeogene (early Tertiary) pollen and spore spectra from north-west Europe allows the identification of four major groups of taxa¹. Three are thought to include the Palaeogene equivalents of taxa now found in deciduous forest, fern and conifer forest and paratropical rain forest. The other is a rubbish-bin of plant taxa reflecting the influences of transport and catchment processes. We have disentangled these effects from the ecological processes and, by analogy with plant megafossil evidence, obtained estimates of summer maximum and winter minimum temperatures, as well as estimates of mean annual temperatures. The resulting picture of climatic fluctuations in the Palaeogene can be recognized in localities throughout north-west Europe. We show here that the general similarity to results of oxygen isotope analyses from deep-sea cores² and the North Sea³ suggests that genuine global climatic changes are being detected. Major differences between 'Oligocene' and 'Eocene' climates are also suggested by these reconstructions and support conclusions from other evidence⁴.

At the heart of our study were detailed quantitative analyses of 187 samples containing 85 palynological form-genera from three boreholes (Ramnor, Bunker's Hill and Shamblehurst Lane) in the Hampshire Basin of southern England. These span most of the Eocene from the bottom of the London Clay to near the top of the Headon Beds⁵. The boreholes are in what is believed to have been mainly a shallow-water marine area, perhaps 10–20 km from the coast. A wide range of sedimentary environments appear to have been sampled—marine, brackish, estuarine and lagoonal. 'Principal components analysis' of the pollen percentages identified 31 non-trivial associations of taxa of which 20 (after variable-maximizing rotation and cluster analysis of the original correlation matrix) could be readily interpreted in ecological terms, while the remaining 11 were enigmatic or described groups of pollen taxa that were clearly

associated with catchment regimes rather than ecology⁶. For instance, the association of *Graminidites*, *Milfordia* and *Spar-ganiaceapollenites* in the same principal component is strongly suggestive of a marsh community, and because some of the other associated taxa have been compared with tropical forest plants, an analogy to swamps found in tropical river deltas today can be suggested. The relative clarity of the distinction between catchment-related and ecologically informative principle components may be a result of the length of the chronological period considered, or of the heterogeneity of the sediments sampled, or a combination of both features.

Our recent study of these 20 ecologically informative rotated principal components suggested that they could be sorted into three major taxonomic groups having ecological significance: deciduous forest, fern and conifer forest and paratropical rain forest¹. Figure 1 illustrates the dendrogram produced by the average-method clustering of the original correlation matrix. It indicates the gross structure of the matrix, and reveals similar groupings to those defined by principal components analysis. The composition of the three groups invited comparison with Wolfe's leaf physiognomic classifications of extant⁷ and extinct⁸ floras, and are consistent with the relationships to modern plant families proposed by Muller⁹. The stratigraphical distribution of these three different groups of principal components is reflected in the pollen diagrams of Fig. 2. The principal components of group III (paratropical rain forest affinity) appear to be of major importance in the uppermost London Clay and basal Headon Beds, while above this, principal components of group I pollen (related to modern deciduous forests) play a major part.

Similar calculations have now been made for other palynological data from the Oligocene of the western British Isles^{10,11}, and the Tertiary of the Paris Basin¹² and the Armorican Massif¹³. The results suggest that our equations are valid and applicable far outside the geographical and chronological range for which they were designed. These results are shown in Fig. 2 which represents the first objective and quantitative palynological historical record of Palaeogene Europe.

The traditional methods of palaeopalynological biostratigraphical correlation depend on the presence or absence of pollen types having stratigraphically limited ranges. There are 28 pollen taxa known to have restricted chronological distributions in the Eocene of southern Britain¹⁴, by means of which